

Stepwise Regression and Pre-trained Edge for Robust Stereo Matching

Weiying Xiao, Wei Zhao*

Abstract—Due to the difficulty in obtaining real samples and ground truth, the generalization performance and the fine-tuned performance are critical for the feasibility of stereo matching methods in real-world applications. However, the diverse datasets exhibit substantial discrepancies in disparity distribution and density, thus presenting a formidable challenge to the generalization and fine-tuning of the model. In this paper, we propose a novel stereo matching method, called SR-Stereo, which mitigates the distributional discrepancies across different datasets by predicting the disparity clips and uses a loss weight related to the regression objective scale to improve the accuracy of the disparity clips. Moreover, this stepwise regression architecture can be easily extended to existing iteration-based methods to improve the performance without changing the structure. In addition, to mitigate the edge blurring of the fine-tuned model on sparse ground truth, we propose Domain Adaptation Based on Pre-trained Edge (DAPE). Specifically, we use the predicted disparity and RGB image to estimate the edge map of the target domain image. The edge map is filtered to generate edge map background pseudo-labels, which together with the sparse ground truth disparity on the target domain are used as a supervision to jointly fine-tune the pre-trained stereo matching model. These proposed methods are extensively evaluated on SceneFlow, KITTI, Middlebury 2014 and ETH3D. The SR-Stereo achieves competitive disparity estimation performance and state-of-the-art cross-domain generalisation performance. Meanwhile, the proposed DAPE significantly improves the disparity estimation performance of fine-tuned models, especially in the textureless and detail regions.

Index Terms—Stereo, robust stereo matching, stepwise regression, domain adaptation

I. INTRODUCTION

DDEPTH information is key to computer vision and graphics research in the real world. Accurate depth estimation is vital for fields such as autonomous driving, robot navigation and action recognition. Common depth estimation methods include structured light [1], stereo matching [2]–[4], radar [5], etc. The structured light method projects a coded pattern onto the object surface and estimates the depth by observing the distortion of the pattern imaged on the object surface. Due to the need to project multiple patterns consecutively, structured light methods are generally only suitable for static indoor scenes. The radar obtains a sparse depth map by transmitting pulses and receiving echoes. Millimeter-wave radar has a long detection range but fuzzy spatial resolution, while laser radar

Corresponding author: Wei Zhao.

Weiying Xiao is with the School of Electronic Information Engineering, Beihang University, Beijing 100191, China, (e-mail: xiaowqtx@buaa.edu.cn)

Wei Zhao is with the School of Electronic Information Engineering, Beihang University, Beijing 100191, China, (e-mail: @buaa.edu.cn)

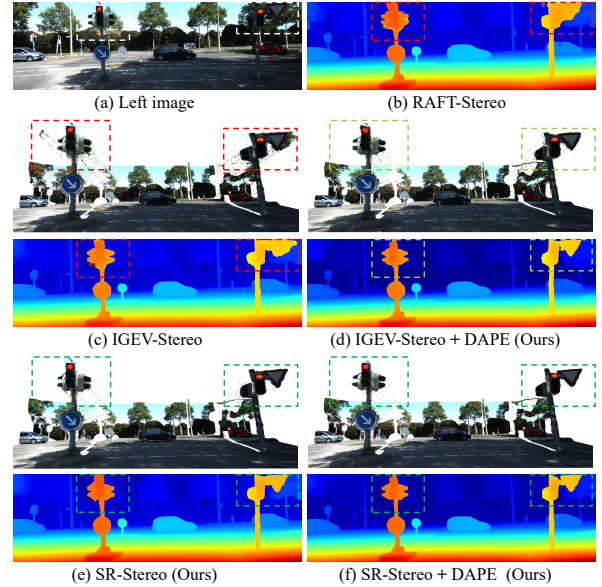


Fig. 1. Domain-adaptive visualization on KITTI. All methods are trained on SceneFlow and fine-tuned on KITTI. During inference, all methods run 15 disparity updates. Our proposed SR-Stereo achieves more accurate performance in the edge region. Meanwhile, as a generalized fine-tuning framework, our proposed DAPE effectively improves the disparity estimation performance of existing methods fine-tuned with sparse ground truth.

has a high spatial resolution but is expensive. In contrast, stereo matching calculates the depth map by estimating the horizontal displacement map (i.e., the disparity) of the pixels between the corrected left and right image pairs. By utilizing only two cameras, stereo matching is able to provide dense depth maps in different scenes, and is therefore considered a cost-effective and widely applicable method for depth estimation.

Many learning-based stereo methods [6]–[12] have achieved encouraging success. Some works [12]–[14] focus on designing the 4D cost volume, which characterizes the cost of pixel matching between left and right image pairs. They use 3D convolutional networks to aggregate and regularize the entire cost volume, and regress it to obtain the disparity. However, the large number of 3D convolutions leads to large computational and memory cost, which limits the applicability of such methods. Recently, iteration-based methods [15]–[22] have shown great potential in terms of both accuracy and real-time performance, and thus have become the mainstay of current research. Iterative-based methods index the similarity features

within current disparity neighborhood from the cost volume and then use it to update the disparity. This approach avoids the expensive cost of aggregating and regularizing cost volume and achieves a balance between performance and efficiency by controlling the number of iterations. In addition, some state-of-the-art iteration-based methods [17], [18] utilize a lightweight 3D convolutional network to regress the coarse initial disparity, thus further accelerating the iteration efficiency.

However, stereo methods usually suffer from the problems of few real samples and difficult access to ground truth in practical applications. Existing methods [23]–[27] are generally pre-trained on a virtual dataset (e.g., SceneFlow [29]) and fine-tuned or directly inferred on real datasets, which imposes higher requirement on the generalization performance. In addition, there are significant discrepancies in disparity distribution and density among different datasets due to variations in acquisition equipment and environment. The Middlebury 2014 [30], which uses hand labeling to obtain dense ground truth, has a maximum disparity value of more than 250 pixels. The KITTI dataset [31], [32], which uses radar and careful calibration to obtain sparse ground truth, has all of its disparities within 100 pixels. These discrepancies make it difficult for a method that performs well on one dataset to directly achieve the same performance on other datasets. Therefore, we need to improve the method so that it has good performance in estimating disparity across domains.

In this paper, we claim that by designing a regression objective with a similar distribution across different datasets, excellent performance can be consistently achieved using the same method across various datasets. Therefore, a disparity stepwise regression (DSR) is proposed to study the disparity estimation in robust stereo matching. Specifically, the regression objective in the DSR is multiple disparity clips, which have the same range across different datasets. By summing the multiple disparity clips, the DSR enables accurate and robust disparity estimation. Meanwhile, a loss weight related to the regression objective scale is proposed to improve the accuracy of disparity clips because it effectively mitigates the long-tailed distribution problem [33], [34] of the disparity clips. Based on these two simple but powerful methods, we design a novel architecture, Stepwise Regression Stereo (SR-Stereo), for robust disparity estimation.

Furthermore, we observe that models fine-tuned with sparse ground truth suffer from severe edge blurring, i.e., edge disparity errors. As shown in Figure 1, even the state-of-the-art models [16], [17] in the KITTI online leaderboard fail to accurately estimate the edge disparity. This further limits the effectiveness of stereo methods in real-world applications, as the vast majority of efficient labeling methods (e.g., radar) can only obtain sparse ground truth. The most direct way to mitigate this problem is to introduce edge-dependent supervision, but current edge feature extraction methods [35]–[40] have difficulty in obtaining accurate and concise edges as pseudo-label due to the overly sparse disparity ground truth and the interference of object textures in RGB images.

In this paper, a Domain Adaptation Based on Pre-trained Edge (DAPE) is proposed to address the issue of blurring in edge details. The two key observations behind this approach

are: 1) disparity has more concise and reliable information about object edges compared to RGB maps. 2) models pre-trained with dense ground truth tend to have accurate edge in predicted disparity on new domains. Therefore, we first propose a lightweight edge estimator that takes both disparity and RGB image as inputs to generate a dense edge map. This estimator, along with SR-Stereo, is pre-trained on a virtual dataset. We utilize the pre-trained SR-Stereo to generate the disparity map for the target domain, which is further fed into the edge estimator to predict the edge map. Then, the background pixels in the edge map are retained and utilized as edge pseudo-label, while the foreground pixels are filtered out. Finally, we use the edge pseudo-label as additional supervision during the model fine-tuning process, which effectively improves the model’s disparity estimation performance on edge details.

In summary, our main contributions are:

- We propose a novel architecture, called SR-Stereo, which predicts disparity clips to alleviate distribution discrepancies across different datasets and uses a loss weight related to the regression objective scale to improve the accuracy of the disparity clips. Experiments on RAFT-Stereo and IGEV-Stereo also demonstrate that the proposed stepwise regression architecture has better generalization performance than iteration-based methods.
- We propose a novel fine-tuning framework for real datasets, named DAPE. By employing generated edge pseudo-label to supervise the model fine-tuning process, our proposed method effectively improves the disparity estimation performance of models fine-tuned with sparse ground truth.
- We perform experiments on SceneFlow, KITTI, Middlebury 2014 and ETH3D. Compared to existing methods, the proposed SR-Stereo achieves the state-of-the-art cross-domain generalization performance across multiple datasets and obtains competitive results on the SceneFlow and KITTI benchmark. Meanwhile, experimental results on multiple realistic datasets show that the proposed DAPE significantly improves the disparity estimation performance of the fine-tuned model, especially in untextured and detailed regions.

II. RELATED WORK

A. Iterative-based Stereo Matching

Compared to cost aggregation-based methods [41]–[43], iteration-based methods achieve significant improvement in both efficiency and accuracy. RAFT-Stereo [16], [44] is the first iteration-based method that constructs cost volume by calculating the dot product of features with same height. At the same time, it introduces multi-level GRU (Gated Recurrent Unit) unit [45] which updates the disparity by indexing the features of cost volume. Based on RAFT-Stereo, DLNR [22] uses decoupled LSTM [46] (Long Short-Term Memory) instead of GRU to retain more high-frequency information during the iteration process, and designs a normalized refinement module to capture more detailed information at full resolution. The refinement of high-frequency information

effectively improves the performance of disparity estimation. Further, CREStereo [15] applies the iterative process to different resolutions of disparity. It uses a deformable search window to more accurately index the features of cost volume, and proposes a hierarchical refinement network to update the disparity at different resolutions in a coarse-to-fine order. In recent research, cost aggregation based on 3D convolutional networks is revisited. For instance, IGEV-Stereo [17] constructs a geometric encoding volume by combining Group-wise correlation and All-pairs Correlation, and uses a lightweight 3D regularization network to regress the initial disparity, which effectively improves the iterative efficiency and accuracy.

Our proposed SR-Stereo is similar in process to the iteration-based methods, but has a different objective. The iteration-based methods focus on how to efficiently converge the disparity, and thus all of its update units target the ground truth disparity. Instead, the proposed SR-Stereo focuses on improving the generalization performance by mitigating the discrepancies in the disparity distribution among different domains. To this end, the update units of SR-Stereo are all individually assigned different objectives, i.e., range-constrained disparity clips.

B. Robust Stereo Matching

Since real samples and ground truth disparity are difficult to obtain for practical applications, some works [26]–[28] focus on cross-domain generalization, which aims to ensure good performance of the model on unseen datasets. CFNet [26] and UCFNet [27] narrow the domain discrepancy by cascaded cost volume and multi-stage refinement of disparity. They also adaptively adjust the search space of disparity at each stage by uncertainty estimation. DSMNet [28] employs domain normalization and a trainable structure-preserving graph-based filter to extract robust geometric feature to improve the cross-domain generalization performance. These methods enhance the generalization performance by improving the network structure. In contrast, our proposed DSR designs a new regression objective with similar distribution across different datasets to reduce the generalization difficulty.

In addition, making good use of the few real samples is important for domain adaptation of the model. Some works [16]–[18] have demonstrated that even using only a few samples, the performance of pre-trained models in a new domain can be significantly improved. However, most existing methods simply employ direct fine-tuning of the model using the ground truth disparity of the new domain, without considering the impact of ground truth density on domain adaptation. For instance, models fine-tuned with sparse ground truth often suffer from severe edge blurring. To address this problem, we propose a domain adaptation based on pre-trained edge which utilizes edge pseudo-label from the target domain to preserve the model’s disparity estimation capability for edge details.

III. METHODOLOGY

A. Framework Overview

In this paper, we propose a novel stereo matching architecture, SR-Stereo, which achieves robust disparity estimation by

stepwise regression of the disparity. In addition, we provide a general and reliable framework, DAPE, for model fine-tuning on sparse ground truth by digging into the disparity-based edge estimation. As shown in Figure 2, the proposed DAPE consists of three steps:

- 1) Firstly, a robust stereo model and a lightweight edge estimator are pre-trained on a large synthetic dataset with dense ground truth. Specifically, a stepwise regression stereo (SR-Stereo) is proposed to mitigate the disparity distribution discrepancies between different datasets. Meanwhile, the disparities predicted by SR-Stereo are fed jointly with the RGB images into a lightweight network to learn the edge information.
- 2) Then, the pre-trained stereo matching model and the edge estimator are used to directly infer on the target domain and generate corresponding edge maps. To mitigate the negative impact of disparity errors in reflective regions, we propose to use only the relatively dense background pixels (i.e., non-edge region pixels) from the edge maps as pseudo-label.
- 3) After generating the edge pseudo-label of the target domain, we use it and the sparse ground truth disparity to jointly fine-tune the pre-trained stereo matching model. Experimental results show that the incorporation of edge pseudo-label supervision significantly improves the disparity estimation performance of the fine-tuned model.

The following subsections describe the proposed SR-Stereo and DAPE in more detail.

B. Stepwise Regression Stereo

Figure 3 shows the overall architecture of the proposed SR-Stereo, which is improved based on the iterative stereo method IGEV-Stereo. Intuitively, the proposed SR-Stereo reconstructs the update unit and the regression objective, and proposes a loss weight related to the regression objective scale to improve the accuracy of disparity clips.

1) *Feature Encoder*: Following IGEV-Stereo, we use MobileNetV2 [47] pre-trained on ImageNet [48] and a series of upsampling blocks to extract multi-scale features $f_1^{left,i} \in \mathbb{R}^{C_i \times H/2^{i+1} \times W/2^{i+1}}$ from the left image $I_{left} \in \mathbb{R}^{3 \times H \times W}$ and $f_1^{right,i} \in \mathbb{R}^{C_i \times H/2^{i+1} \times W/2^{i+1}}$ from the right image $I_{right} \in \mathbb{R}^{3 \times H \times W}$, respectively. The $i=1,2,3,4$ and the feature size $C_i=48,64,192,160$.

2) *Context Encoder*: We use a series of residual blocks [49] and downsampling layers to extract multi-scale context features $f_2^{left,j} \in \mathbb{R}^{C_j \times H/2^{j+1} \times W/2^{j+1}}$ ($j=1,2,3,4$ and $C_j=128$) from the left image. These features are inserted into the stepwise regression unit to provide global information.

3) *Fused Cost Volume*: By combining Group-wise correlation and Correlation, we construct the cost volume G_c based on $f_1^{left,1}$ and $f_1^{right,1}$. Then, we use a lightweight 3D UNet to aggregate the cost volume and obtain the initial disparity $d_{init} \in \mathbb{R}^{1 \times H/4 \times W/4}$.

4) *Disparity Stepwise Regression*: We propose a disparity stepwise regression, which obtains the disparity by predicting multiple disparity clips with the same range. It consists of

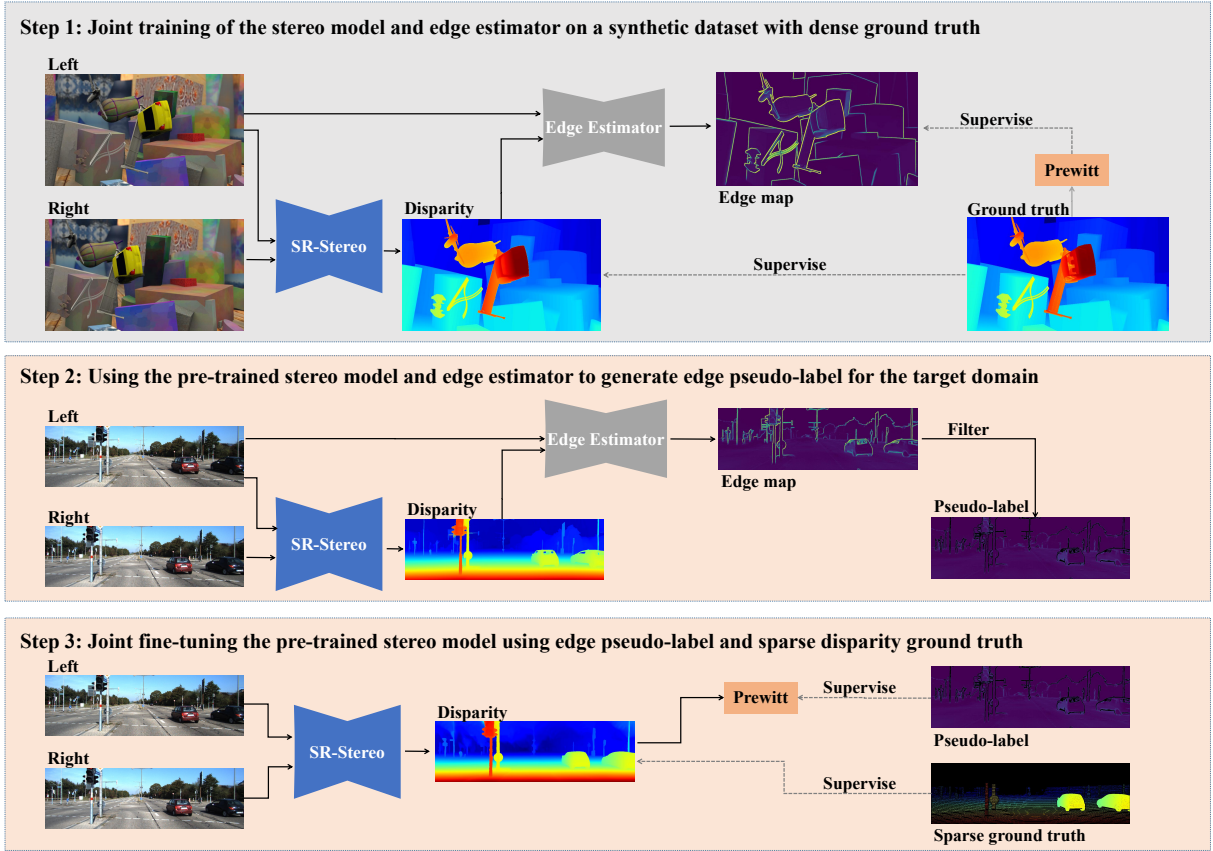


Fig. 2. The overall framework of the proposed DAPE. First, a robust stereo model SR-Stereo and a lightweight edge estimator are pre-trained on a large synthetic dataset with dense ground truth. Then, we use the pre-trained SR-Stereo and edge estimator to generate the edge map of target domain, where the background pixels (i.e., non-edge region pixels) are used as edge pseudo-label. Finally, we jointly fine-tune the pre-trained SR-Stereo using the edge pseudo-label and sparse disparity ground truth.

two parts, including stepwise regression unit and regression objective segmentation.

Stepwise Regression Unit. Figure 4 shows the architecture of the stepwise regression unit. For each regression, we index a set of features f_G from the cost volume G_c using the cumulative disparity-centered set as follows:

$$f_G = \sum_{r=-4}^4 \text{concat} \{G_c(d_k + r), G_c^p(d_k/2 + r)\} \quad (1)$$

where d_k is the cumulative disparity ($d_0 = d_{init}$) and p denotes the average pooling operation. We use these features from G_c along with the cumulative disparity d_k to update the hidden state h_k of ConvGRU [17]:

$$h_{k+1} = \text{ConvGRU}(f_G, d_k, h_k, f_2^{left}) \quad (2)$$

Then, the updated hidden state h_{k+1} and f_G are passed into a series of convolutional layers and residual layers [49] to generate the disparity clip $\Delta d_{k+1} \in \mathbb{R}^{1 \times H/4 \times W/4}$ as follows:

$$w = \sigma(\text{Conv}_{1 \times 1}(\text{Res}(f_G))) \quad (3)$$

$$\Delta d_{k+1} = \tanh\left(\frac{\text{Conv}_{3 \times 3}(\text{Relu}(\text{Conv}_{3 \times 3}(h_{k+1})))}{m}\right) \times m \odot (1 + 0.5w) \quad (4)$$

where σ denotes the sigmoid function, Res is the residual layer, and \odot denotes the Hadamard product. We set the hyperparameter m to constrain the size of the disparity clip and use a weight map w computed from the cost-volume features f_G to adjust the constraint magnitude. Finally, we update the current cumulative disparity and use the Spatial Upsampling [17] to generate the full-resolution cumulative disparity $d_{k+1}^{full} \in \mathbb{R}^{1 \times H \times W}$ as follows:

$$d_{k+1} = d_k + \Delta d_{k+1} \quad (5)$$

$$d_{k+1}^{full} = \text{Upsampling}(f_1^{left, i}, I_{left}, 4d_{k+1}) \quad (6)$$

Regression Objective Segmentation. We specify how to obtain the ground truth disparity clip $\Delta d_{gt, k}$ and the full-resolution ground truth cumulative disparity $d_{gt, k+1}^{full}$. Specifically, the ground truth of the full-resolution cumulative disparity is constantly changing with the stepwise regression process, as shown below:

$$d_{gt, k+1}^{full} = d_k^{full} + \text{clip}_{-6m}^{6m}(d_{gt} - d_k^{full}) \quad (7)$$

in which

$$\text{clip}_{-M}^M(x) = \begin{cases} -M & \text{if } x < -M \\ x & \text{if } -M \leq x \leq M \\ M & \text{if } x > M \end{cases} \quad (8)$$

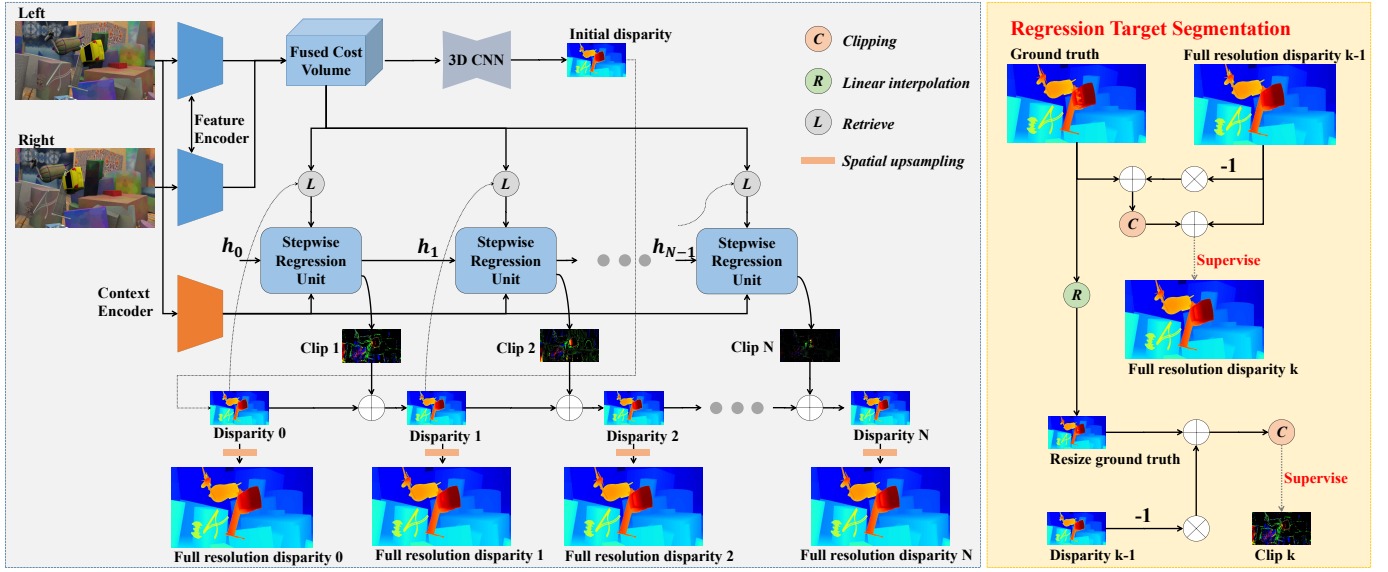


Fig. 3. The overall architecture of the proposed SR-Stereo. Compared to iteration-based methods, SR-Stereo is specially designed in terms of the update unit and the regression objective. Specifically, a stepwise regression unit is proposed to control the range of disparity clips. Accordingly, a regression objective segmentation is proposed to design a separate regression objective for each stepwise regression unit.

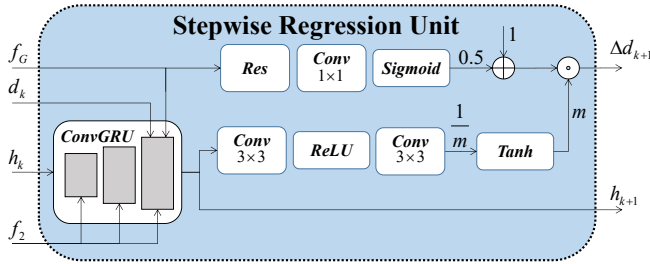


Fig. 4. Architecture of the stepwise regression unit. The m is the hyperparameter that controls the range of the output disparity clip.

where d_{gt} is the ground truth disparity and $clip$ denotes the clipping operation.

In addition, we use linear interpolation to generate the ground truth disparity clip $\Delta d_{gt,k}$:

$$\Delta d_{gt,k} = clip_{-1.5m}^{1.5m} \left(\frac{Resize(d_{gt})}{4} - d_k \right) \quad (9)$$

where $Resize$ denotes linear interpolation downsampling.

5) *Disparity Clip-Balanced Weight*: In SR-Stereo, the regression disparity is divided into multiple clips with the same range to mitigate the distributional discrepancies among different domains. Ideally, a regression disparity of size L is split into a number of disparity clips of size $1.5m$ and a small disparity clip of size n as follows:

$$L = k \times 1.5m + n \quad (10)$$

where $k \in \mathbb{Z}$ and $n \in (0, 1.5m)$. When the initial disparity is far from the ground truth disparity (i.e., L is large), the distribution of disparity clips is long-tailed, which limits the accuracy of small disparity clip. In this paper, a Disparity Clip-Balanced Weight is proposed to mitigate the long-tailed

distribution of disparity clips. The formula for this weight is as follows:

$$w_{balanced}(x) = clip_0^{1.5} (|x|^{-h}) \quad (11)$$

where h is a hyperparameter that controls the bias towards small disparity clip. This weight can be flexibly inserted into existing loss functions:

$$CB_{L1}(x) = w_{balanced}(x) \times |x| \quad (12)$$

$$CB_{SmoothL1}(x) = \begin{cases} w_{balanced}(x) \times 0.5x^2 & \text{if } x < 1 \\ w_{balanced}(x) \times |x| & \text{otherwise} \end{cases} \quad (13)$$

6) *Loss Function*: We use Smooth L1 loss to supervise the initial disparity and the disparity clips d_k because it is more sensitive to large errors:

$$Loss_{init} = Smooth_{L1}(d_{init}^{full} - d_{gt}) \quad (14)$$

$$Loss_{\Delta d} = \sum_{k=1}^N \gamma^{N-k} CB_{SmoothL1}(\Delta d_k - \Delta d_{gt,k}) \quad (15)$$

where $\gamma = 0.9$ and N is the total number of disparity clips. We use L1 loss to supervise full-resolution cumulative disparity:

$$Loss_{full} = \sum_{k=1}^N \gamma^{N-k} CB_{L1}(d_k^{full} - d_{gt,k}^{full}) \quad (16)$$

Ultimately, the total loss function for SR-Stereo is as follows:

$$Loss_{total} = Loss_{init} + Loss_{\Delta d} + Loss_{full} \quad (17)$$

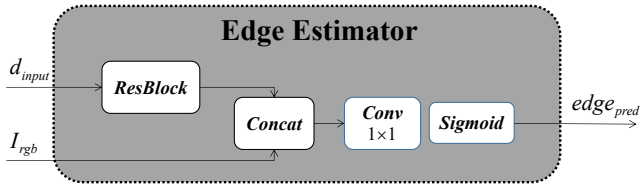


Fig. 5. Architecture of the edge estimator. The entire architecture consists of only one residual block and one convolution block.

7) *Generalization of the stepwise regression architecture:* We observe that although the core idea is different, the stepwise regression architecture is similar to existing iteration-based methods in terms of processing flow, and thus can be easily generalized based on existing methods. In Section IV-D, we also apply the proposed stepwise regression architecture to the classic iteration-based method RAFT-Stereo, and the experimental results also show that the stepwise regression architecture performs better.

C. Domain Adaptation Based on Pre-trained Edge

We propose a Domain Adaptation Based on Pre-trained Edge (DAPE) to mitigate edge blurring for model fine-tuned with sparse ground truth. Specifically, a lightweight edge estimator is proposed to generate edge map of the target domain image, which is filtered to generate the edge map background pseudo-label. This pseudo-label, along with the sparse ground truth disparity in the target domain, are utilized as supervision to jointly fine-tune the pre-trained stereo matching model. In the following, we describe the edge estimator, the edge map background pseudo-label and the joint fine-tuning process in detail.

1) *Edge Estimator:* For the proposed DAPE, the reliability of edge pseudo-label is vital to the performance of the fine-tuned model. Existing edge estimation methods usually take only an RGB image as input and use a series of complex 2D CNNs to estimate the contour of object by extracting high-level features. However, this approach significantly increases the computational cost and limits the generalization performance due to the large discrepancies in object classes among different domains.

In this paper, we claim that using disparity for edge estimation is a better and more robust approach because disparity estimation focuses on local geometric information, whose representations are similar across domains. Moreover, compared to RGB image, disparity contains almost no object texture information, which greatly reduces the difficulty of edge estimation. Thus, a lightweight edge estimator is proposed to achieve accurate and robust performance by introducing disparity. The architecture of the edge estimator is shown in Figure 5. First, a residual block is used to extract the edge feature in the disparity:

$$f_{edge} = ResBlock(d_{input}) \quad (18)$$

where $ResBlock$ denotes the residual block, d_{input} is the disparity, and the number of channels for f_{edge} is 29. In order

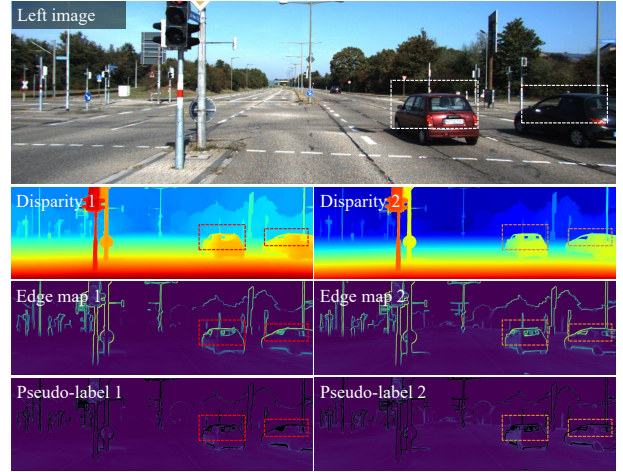


Fig. 6. Generalization results of existing methods on KITTI 2015. The labels 1 and 2 in the figure denote the IGEV-Stereo and the proposed SR-Stereo, respectively. The edge map is represented using a pseudo-color image, where the black color indicates the invalid regions. As shown, the existing methods perform poorly in reflective regions, which leads to wrong edges. Therefore, we propose to use only pixels in non-edge region as pseudo-label.

to mitigate the potential effects of noise in the disparity, the RGB image is used to refine the edge feature map. Specifically, the edge feature and the corresponding RGB image are passed together to a residual block to achieve feature refinement. Finally, we use a 1×1 convolutional layer and a sigmoid layer to generate the refined edge map as follows:

$$f_{refine} = ResBlock(concat(f_{edge}, I_{rgb})) \quad (19)$$

$$edge_{pred} = \sigma(Conv_{1 \times 1}(f_{refine})) \quad (20)$$

where $edge_{pred}$ is the predicted edge map, I_{rgb} is the RGB image corresponding to the disparity, σ denotes the sigmoid function, and the number of channels of f_{refine} is 16.

Loss Function. We use Smooth $L1$ loss to train the proposed edge estimator on a large synthetic dataset:

$$Loss_{edge} = Smooth_{L1}(edge_{pred} - edge_{gt}) \quad (21)$$

where $edge_{gt}$ is the ground truth edge map. Since the ground truth edge map is not provided in the dataset, we use the Prewitt operator to extract the edge of the ground truth disparity as $edge_{gt}$:

$$edge_{gt} = \begin{cases} 1 & \text{if } Prewitt(d_{gt}) > 5 \\ 0 & \text{otherwise} \end{cases} \quad (22)$$

where d_{gt} is the ground truth disparity and $Prewitt$ denotes the Prewitt operator.

2) *Edge Map Background Pseudo-label Generation for Target Domain:* The proposed edge estimator achieves edge estimation by introducing disparity, and therefore is affected by the accuracy of the disparity. As shown in Figure 6, existing disparity estimation methods perform badly in reflection regions, which leads to erroneous edges. In this paper, an edge map background pseudo-label is proposed to generate reliable supervision for fine-tuning. Intuitively, in an ideal edge map, both the edge region and non-edge region can

be leveraged as supervision to improve the performance of the fine-tuned disparity estimation model. For instance, the disparity map typically exhibits high gradients in edge region, while it remains relatively flat in non-edge region. Erroneous edges in reflection regions do not affect the reliability of the pixels in the non-edge region. Therefore, we can simply utilize pixels in non-edge region as the pseudo-label (i.e., the edge map background pseudo-label):

$$edge_{background} = \{p < t \mid p \in edge_{pred}\} \quad (23)$$

where t is the threshold that controls the density of non-edge region.

3) *Joint Fine-tuning on the Target Domain*: After obtaining the edge map background pseudo-label, we use it and the sparse ground truth disparity from the target domain as supervision to jointly fine-tune the pre-trained stereo matching model. Specifically, we propose an edge-aware loss to improve the detail of the predicted disparity as follows:

$$Loss_{edge} = Smooth_{L1}(edge_{d_{pred}} - edge_{background}) \quad (24)$$

where $edge_{d_{pred}}$ is the edge map corresponding to predicted disparity d_{pred} . As in Section III-C1, we use the Prewitt operator to extract the edge map of the predicted disparity:

$$edge_{d_{pred}} = \sigma(10 \times (Prewitt(d_{pred}) - 5)) \quad (25)$$

The total loss of the joint fine-tuning process is shown below:

$$Loss_{DAPE} = Loss_{stereo} + Loss_{edge} \quad (26)$$

where $Loss_{stereo}$ is the loss of the original stereo matching method, e.g., Eq 17.

IV. EXPERIMENTS

A. Datasets and Evaluation Metrics

SceneFlow [29] is a large synthetic dataset that consists of 35,454 training pairs and 4,370 testing pairs, with a resolution of 960×540 . It provides dense ground truth for optical flow and stereo matching. We utilize this dataset to pretrain the proposed SR-Stereo and the edge estimator with 3-pixel error and end-point error (EPE) as evaluation metrics.

Middlebury 2014 [30] consists of two batches of indoor image pairs. The first batch provides 15 training pairs and 15 test pairs, with each scene provided in three different resolutions. The second batch provides 13 additional training pairs, but contains only one resolution. All training pairs are provided with dense hand-labeled ground truth disparity, which ranges from 0 to 300. We directly use the training pairs from the first batch to evaluate the generalization performance of SR-Stereo. For DAPE, we utilize the additional 13 image pairs to fine-tune the model and evaluate its performance using the 15 training pairs from the first batch. The evaluation metric used is the 2-pixel error.

ETH3D [50] is a grayscale image dataset that includes a variety of indoor and outdoor scenes. It consists of 27 training pairs and 20 test pairs. The dataset provides sparsely labeled ground truth disparities for the training pairs, ranging from 0 to 60 (the smallest among several datasets). Similar to the usage in Middlebury 2014, we employ the training pairs to directly

assess the generalization performance of the proposed method, using the 1-pixel error as the evaluation metric. Additionally, we use 14 training pairs as fine-tuning samples and 13 training pairs as test samples to evaluate the effectiveness of the proposed Domain Adaptation Based on Pre-trained Edge.

KITTI 2012 [32] and **KITTI 2015** [31] are datasets of real-world driving scenes. KITTI 2012 consists of 194 training pairs and 195 test pairs, while KITTI 2015 contains 200 training pairs and 200 test pairs. Both datasets provide sparse ground truth disparity (sparsest in several datasets) obtained using lidar. The disparity values range from 0 to 230. In this paper, we combine KITTI 2012 and KITTI 2015 datasets into a unified dataset referred to as **KITTI**. For evaluation, we adopt the 3-pixel error as the metric. To assess the efficacy of our proposed DAPE method, we allocate 80% of the KITTI training set for fine-tuning the model and reserve the remaining 20% for validation purposes.

B. Implementation Details

In this paper, we implement the proposed methods using pytorch and conduct experiments using two NVIDIA RTX 3090 GPUs. For all the experiments, we use the AdamW optimizer and one-cycle learning rate schedule, as well as the same data augmentation strategies. Specifically, we preprocess the training pairs by applying the saturation transform and randomly cropping them to ensure a consistent image size (320×512 for ETH3D, 384×1024 for Middlebury 2014, and 320×672 for other datasets). Below, we provide a detailed description of the training settings for SR-Stereo and DAPE, respectively.

1) *SR-Stereo*: All ablation versions of SR-Stereo are trained on SceneFlow with a batch size of 4 for 50k steps, while the final version of SR-Stereo is trained on SceneFlow with a batch size of 8 for 200k steps. The final model and ablation experiments are conducted using a one-cycle learning rate schedule with learning rates of 0.0002 and 0.0001, respectively. We evaluate the generalization performance of the proposed method by directly testing on the 27 training pairs from ETH3D and the 15 training pairs from Middlebury 2014.

2) *DAPE*: For the experiments related to the edge estimator, we jointly train the stereo model and the proposed edge estimator on SceneFlow with a batch size of 4 for 50k steps, using a one-cycle learning rate schedule with a learning rate of 0.0001. We use the pre-trained stereo model and edge estimator to generate edge pseudo-labels for target domains. Following existing methods [15], [16], [22], we adopt different settings of fine-tuning process for different datasets. For the KITTI, we adopt a batch size of 4 and fine-tune the model for 50k steps with an initial learning rate of 0.0001. As for the ETH3D, we use a batch size of 2 and fine-tune the model for 2,000 steps, also with an initial learning rate of 0.0001. In the case of the Middlebury 2014, we utilize a batch size of 2 and fine-tune the model for 4,000 steps, starting with an initial learning rate of 0.00002.

C. Ablation Study

In this section, we explore the effectiveness and optimal configuration of each component of SR-Stereo. Additionally,

TABLE I

ABLATION STUDY OF DSR. THE BASELINE IS IGEV-STEREO. ALL METHODS RUN 15 DISPARITY UPDATES DURING INFERENCE. THE num_{GRU} DENOTES THE USAGE TIMES OF CONVGRU, WHILE THE num_{SRU} DENOTES THE USAGE TIMES OF THE PROPOSED STEPWISE REGRESSION UNIT. THE FINAL CONFIGURATION OF m IS UNDERLINED. **BOLD**: BEST.

Experiments	Variations				SceneFlow		Middlebury-H	ETH3D	Params.(M)
	num_{GRU}	num_{SRU}	m	$Loss_{\Delta d}$	EPE(px)	$> 3px$	$> 2px(\%)$	$> 1px(\%)$	
Baseline	15	0	-	-	0.72	3.65	8.44	4.49	12.60
Range of Disparity Clip	0	15	1	-	0.71	3.61	8.42	4.10	12.77
	0	15	2	-	0.69	3.51	7.89	4.47	12.77
	0	15	3	-	0.70	3.55	7.66	4.44	12.77
	0	15	4	-	0.69	3.54	7.31	5.14	12.77
Supervision of Disparity Clip	0	15	<u>2</u>	✓	0.70	3.49	6.78	4.05	12.77
	0	15	3	✓	0.69	3.49	7.44	4.15	12.77
Stepwise Regression Unit (SRU)	4	11	2	✓	0.69	3.49	7.50	4.61	12.77
	4	11	3	✓	0.70	3.56	7.80	4.61	12.77
	8	7	2	✓	0.69	3.49	7.77	4.10	12.77
	8	7	3	✓	0.70	3.52	7.91	4.79	12.77

we apply the proposed stepwise architecture to existing methods to demonstrate its superiority in estimation performance and generalization performance.

1) *Disparity Stepwise Regression*: We explore the optimal settings for DSR as well as its effectiveness. Table I shows the results of DSR in different configurations. In the majority of configurations, the incorporation of DSR significantly enhances the performance of the baseline model across different datasets.

Firstly, experiments conducted with varying ranges (m) of disparity clips demonstrate that the choice of disparity clip range impacts the generalization performance on different datasets. For datasets with a small range of disparity, smaller disparity clips are preferred, while datasets with a larger range of disparity benefit from larger disparity clips. Interestingly, the DSR method achieves consistent and stable performance across all datasets when $m = 2$.

Secondly, our method achieves further performance improvement through the supervision of disparity clips. By incorporating supervision specifically on disparity segments, the model’s accuracy and generalization capability are enhanced.

Furthermore, we investigate the impact of the number of stepwise regression units employed in the architecture. Experimental results reveal that increasing the usage times of stepwise regression units leads to better generalization performance of the model.

2) *Optimal Configuration of Disparity Clip-Balanced Weight*: We explore the optimal configuration of Disparity Clip-Balanced Weight. As shown in Table II, the utilization of Disparity Clip-Balanced Weight significantly improves the performance on multiple datasets. We observe that when the disparity is split into multiple clips, the imbalance problem is shifted from the distribution of disparity between different domains to the distribution of disparity clips within the same domain. Therefore, our proposed DSR and Disparity Clip-Balanced Weight is an effective combination for achieving excellent cross-domain generalization performance.

3) *Number of Stepwise Regression Units*: Similar to the iteration-based methods, our SR-Stereo can trade off efficiency and performance by adjusting the number of update units. As shown in Table III, SR-Stereo can achieve better performance for the same number of updates compared to the best iteration-

TABLE II

ABLATION STUDY OF DISPARITY CLIP-BALANCED WEIGHT. WE INTERPOLATE THE PROPOSED DISPARITY CLIP-BALANCED WEIGHT INTO THE LOSS FUNCTION OF SR-STEREO. ALL METHODS RUN 15 DISPARITY UPDATES DURING INFERENCE. THE FINAL CONFIGURATION OF THE h IS UNDERLINED. **BOLD**: BEST.

Methods	h	SceneFlow		Middlebury-F	ETH3D
		EPE(px)	$> 3px$	$> 2px$	$> 1px$
IGEV-Stereo	-	0.72	3.65	17.47	4.49
SR-Stereo	-	0.70	3.49	14.99	4.05
	0.1	0.69	3.44	14.74	3.93
	0.3	0.69	3.32	14.90	4.18
	<u>0.5</u>	0.70	3.23	14.23	3.82

TABLE III

COMPARISON OF THE EFFICIENCY OF DISPARITY UPDATE UNITS ON DIFFERENT ARCHITECTURES. COMPARED WITH IGEV-STEREO, THE PROPOSED SR-STEREO ACHIEVES SIGNIFICANTLY BETTER DISPARITY ESTIMATION AND CROSS-DOMAIN GENERALIZATION WITH THE SAME NUMBER N OF UPDATES. **BOLD**: BETTER.

Methods	N	SceneFlow		Middlebury-H	ETH3D
		EPE(px)	$> 3px$	$> 2px$	$> 1px$
IGEV-Stereo	9	0.73	3.69	8.89	4.74
SR-Stereo		0.72	3.32	7.66	3.93
IGEV-Stereo	12	0.72	3.65	8.59	4.57
SR-Stereo		0.71	3.26	7.31	3.93
IGEV-Stereo	15	0.72	3.65	8.44	4.49
SR-Stereo		0.70	3.23	7.17	3.82
IGEV-Stereo	18	0.71	3.63	8.40	4.43
SR-Stereo		0.70	3.22	7.22	3.86
IGEV-Stereo	21	0.71	3.63	8.44	4.42
SR-Stereo		0.70	3.22	7.15	3.81
IGEV-Stereo	32	0.73	3.68	8.18	4.44
SR-Stereo		0.71	3.24	7.14	3.85

based method, IGEV-Stereo. It also shows that the range constraint on the update units does not reduce the convergence speed of the disparity, but rather makes the updated disparity more accurate.

D. Extension of the stepwise regression architecture

To further demonstrate the superiority of the stepwise architecture for disparity estimation and cross-domain generalization, we retain the existing update unit ConvCRU and apply the proposed Regression Objective Segmentation and Disparity Clip-Balanced Weight to the iteration-based methods RAFT-Stereo and IGEV-Stereo.

TABLE IV
 QUANTITATIVE EVALUATION ON SCENEFLOW AND KITTI. OUR SR-STEREO RUN 32 DISPARITY UPDATES DURING INFERENCE. **BOLD**: BEST.

Method	SceneFlow	KITTI 2015			KITTI 2012						Run-time(s) on KITTI
		D1-bg	D1-fg	D1-all	2-noc	2-all	3-noc	3-all	EPE-noc	EPE-all	
CREStereo [15]	-	1.45	2.86	1.69	1.72	2.18	1.14	1.46	0.4	0.5	0.41
DLNR [22]	0.48	1.37	2.59	1.76	-	-	-	-	-	-	0.28
Croco-Stereo [21]	-	1.38	2.65	1.59	-	-	-	-	-	-	0.93
UPFNet [27]	-	1.38	2.85	1.62	1.67	2.17	1.09	1.45	0.4	0.5	0.25
PSMNet [12]	1.09	1.86	4.62	2.32	2.44	3.01	1.49	1.89	0.5	0.6	0.41
GANNet [41]	0.80	1.48	3.46	1.81	1.89	2.50	1.19	1.60	0.4	0.5	1.80
GwcNet [13]	0.98	1.74	3.93	2.11	2.16	2.71	1.32	1.70	0.5	0.5	0.32
AcfNet [42]	0.87	1.51	3.80	1.89	1.83	2.35	1.17	1.54	0.5	0.5	0.48
ACVNet [14]	0.48	1.37	3.07	1.65	1.83	2.35	1.13	1.47	0.4	0.5	0.20
RAFT-Stereo [16]	0.56	1.58	3.05	1.82	1.92	2.42	1.30	1.66	0.4	0.5	0.38
IGEV-Stereo [17]	0.47	1.38	2.67	1.59	1.71	2.17	1.12	1.44	0.4	0.4	0.18
SR-Stereo(ours)	0.45	1.37	2.49	1.56	1.66	2.07	1.09	1.36	0.4	0.4	0.19

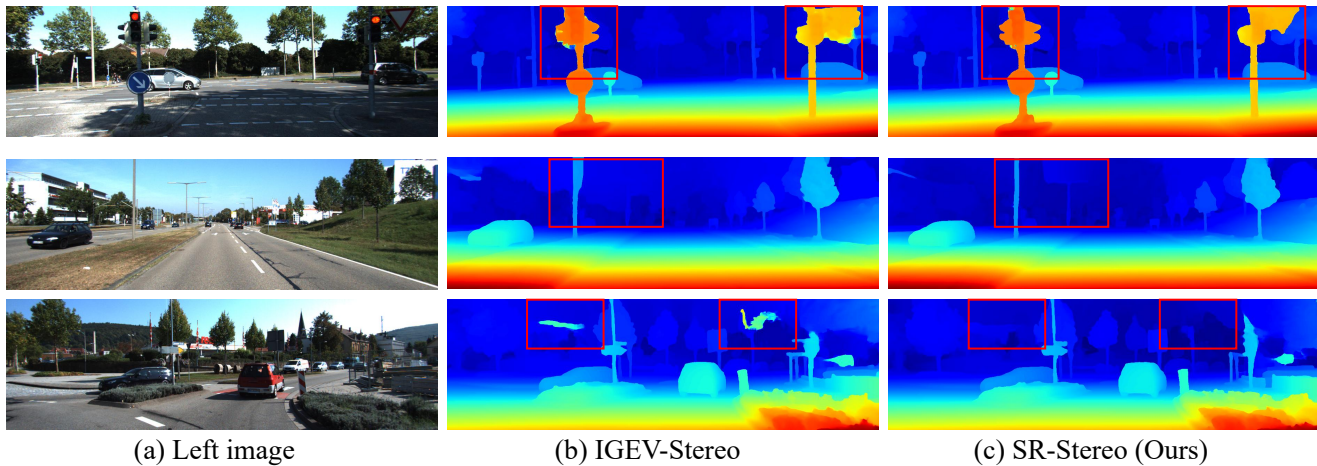


Fig. 7. Qualitative results on the test set of KITTI 2015. Both methods run 32 updates at inference. Our SR-Stereo is more accurate for edge regions and backgrounds.

TABLE V
 EXTENSION RESULTS FOR THE STEPWISE REGRESSION ARCHITECTURE. FOR INFERENCE, IGEV-STEREO RUNS 15 DISPARITY UPDATES, WHILE RAFT-STEREO RUNS 32 DISPARITY UPDATES. ROS:REGRESSION OBJECTIVE SEGMENTATION. DCB: DISPARITY CLIP-BALANCED WEIGHT ($h=0.5$). GRAY: PERFORMANCE IS IMPROVED AFTER USING THE PROPOSED METHOD. **BOLD**: BEST.

Methods	m	SceneFlow > 3px(%)	Middlebury-H > 2px(%)	ETH3D > 1px(%)
IGEV-Stereo	-	3.65	8.44	4.49
IGEV.+ROS	2	3.50	8.09	4.40
	3	3.48	8.06	4.71
	4	3.48	8.10	4.37
IGEV.+ROS+DCB	2	3.32	7.68	3.87
	3	3.26	7.61	4.22
	4	3.24	7.78	3.47
RAFT-Stereo	-	3.96	14.71	4.51
RAFT.+ROS	3	4.25	15.78	3.86
	4	4.01	14.42	4.02
	5	3.76	12.26	4.13
RAFT.+ROS+DCB	3	3.70	13.97	3.60
	4	3.56	12.64	3.63
	5	3.42	11.88	3.59

As shown in Table V, the proposed method can improve the performance of existing iteration-based methods without changing the network structure. In addition, we can adjust the

disparity clip range m to achieve better results according to the characteristics of the existing methods. For instance, in the case of RAFT-Stereo, where the initial disparity is set to 0, a large clip range is required to accelerate the disparity convergence. Therefore, the best results are obtained with a clip range of $m=5$. Conversely, IGEV-Stereo obtains a coarse initial disparity through 3D-CNN, making a smaller clip range more suitable to achieve stable performance improvement.

E. Comparison with SOTA Methods

1) *Benchmark Results*: In this section, we compare SR-Stereo with the state-of-the-art methods published on SceneFlow and KITTI. As described in Section IV-B1, we train the final version of SR-Stereo on SceneFlow. For the KITTI model, we fine-tune the final SceneFlow version of SR-Stereo for 50k steps. Tables IV shows the quantitative results. With similar training strategies, SR-Stereo achieves a new SOTA EPE on the SceneFlow test set. Evaluation results on the KITTI benchmark show that SR-Stereo achieves the best performance on the vast majority of metrics. Figure 7 shows a comparison of the qualitative results of SR-Stereo and IGEV-Stereo on KITTI 2015. Our method is more accurate for edge regions and backgrounds.

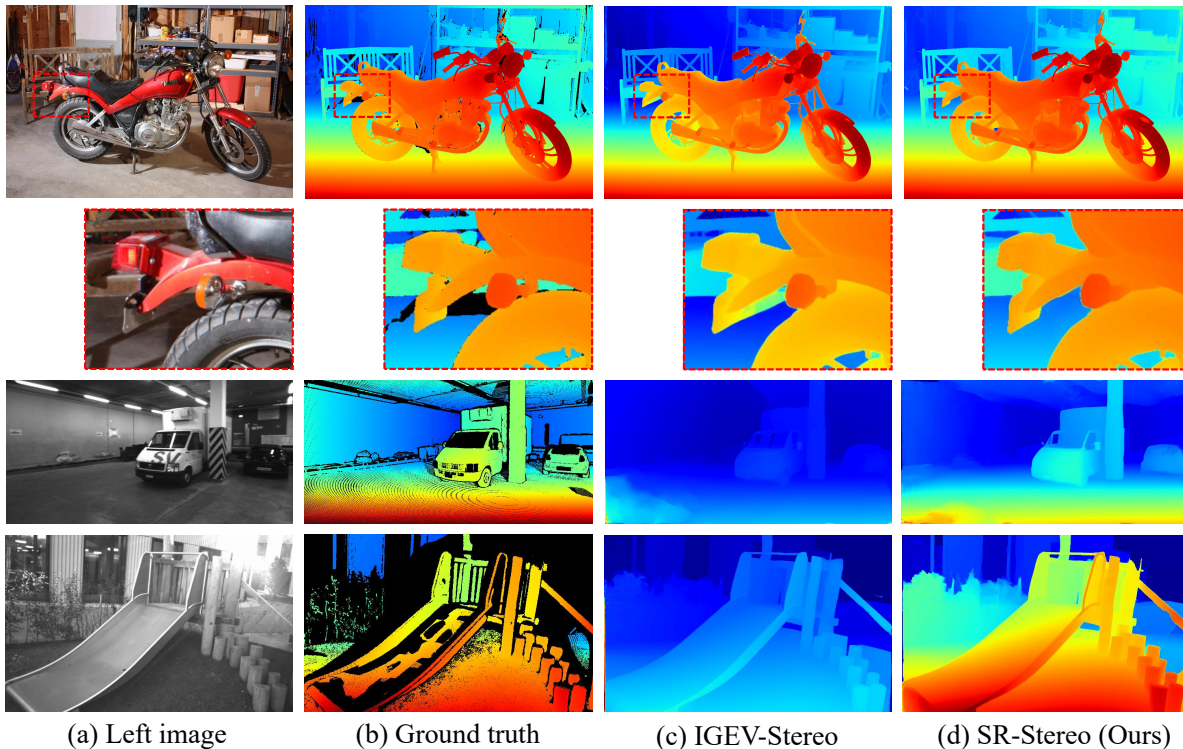


Fig. 8. Generalization results on Middlebury 2014 and ETH3D. All methods run 32 disparity updates during inference. As can be seen from the overall range of the disparity maps, our results are closer to the ground truth and show stronger generalization performance.

TABLE VI
SYNTHETIC DATA GENERALIZATION EXPERIMENTS. THE SR-STEREO RUN 32 DISPARITY UPDATES DURING INFERENCE. WE PRE-TRAIN OUR MODEL ON SCENEFLOW AND TEST IT DIRECTLY ON MIDDLEBURY 2014 AND ETH3D. THE 2-PIXEL ERROR RATE IS USED FOR MIDDLEBURY 2014, AND 1-PIXEL ERROR RATE FOR ETH3D. **BOLD: BEST.**

Method	Middlebury		ETH3D
	half	quarter	
PSMNet [12]	15.8	9.8	10.2
GANNet [41]	13.5	8.5	6.5
DSMNet [28]	13.8	8.1	6.2
STTR [7]	15.5	9.7	17.2
CFNet [26]	15.3	9.8	5.8
RAFT-Stereo [16]	8.7	7.3	3.2
IGEV-Stereo [17]	7.1	6.2	3.6
SR-Stereo(ours)	6.07	6.0	3.0

2) *Zero-shot Generalization:* We test the final SceneFlow version of SR-Stereo directly on Middlebury 2014 and ETH3D. As shown in Table VI, Our SR-Stereo achieves very competitive generalisation performance. Compared with the SOTA method IGEV-Stereo, our method achieves an overall improvement. The qualitative results are shown in Figure 8. As can be seen from the overall range of the disparity maps, our results are closer to the ground truth and show stronger generalization performance.

F. Domain Adaptation Based on Pre-trained Edge

As mentioned in Section III-A, in addition to proposing a robust network SR-Stereo, we also propose the DAPE to

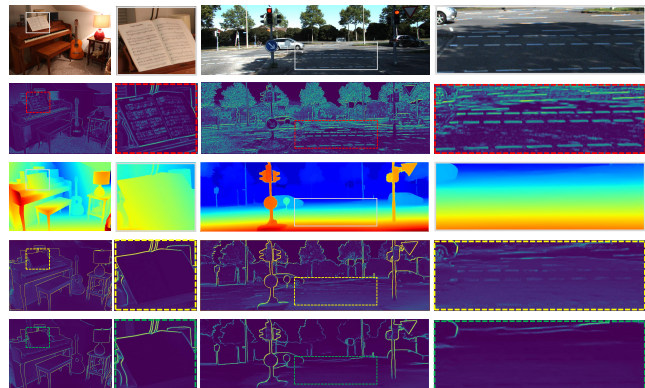


Fig. 9. Edge Estimation Results for Different Inputs. From top to bottom: left RGB image, predicted edge map from the input of the left RGB image, disparity, predicted edge map from the concatenation of the left RGB image and disparity as a four-channel input, predicted Edge Map using our disparity estimator (see details in Figure 5). All methods are trained on the SceneFlow using the same network architecture (i.e., two residual blocks). Test samples are obtained from Middlebury 2014 and KITTI-2015.

enhance the performance of existing models after being fine-tuned with sparse ground truth. In this section, we comprehensively evaluate the individual steps of DAPE and demonstrate its effectiveness through experimental results on KITTI, Middlebury and ETH3D.

1) *Different Inputs to the Edge Estimator:* We explore the impact of different inputs on performance while utilizing the same edge estimator structure. Figure 9 shows the qualita-

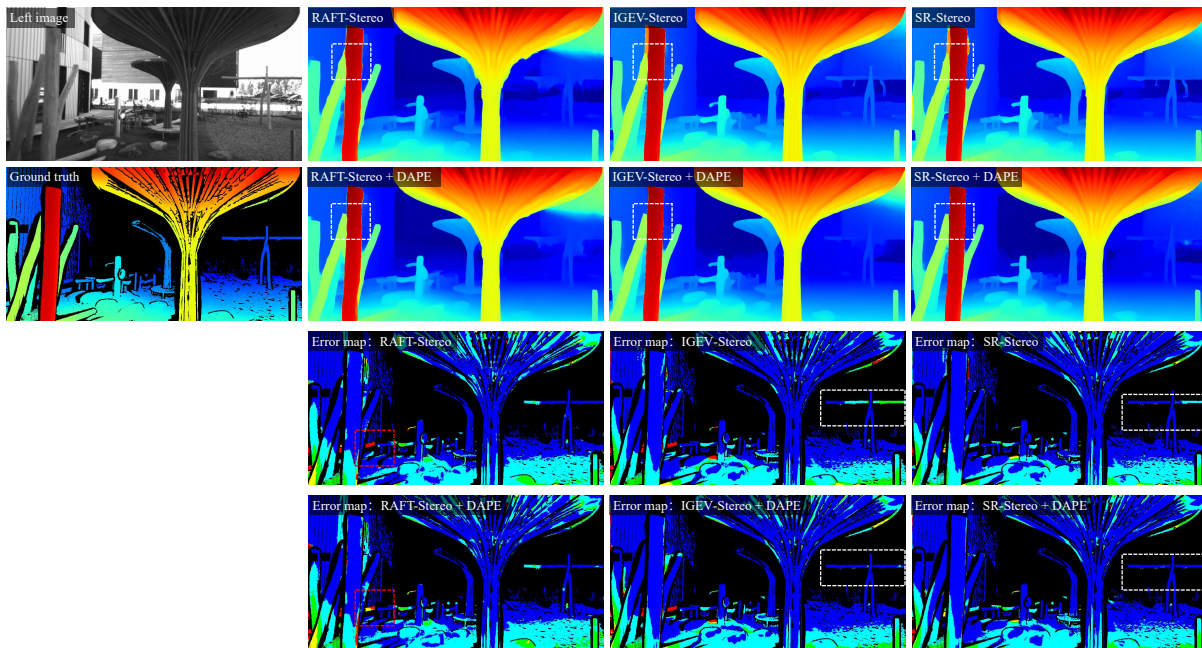


Fig. 10. Qualitative disparity estimation results of DAPE on ETH3D. All methods run 15 disparity updates during inference. The threshold t in DAPE is 0.25. In the error maps, red represents a larger error, while dark blue indicates a smaller error.

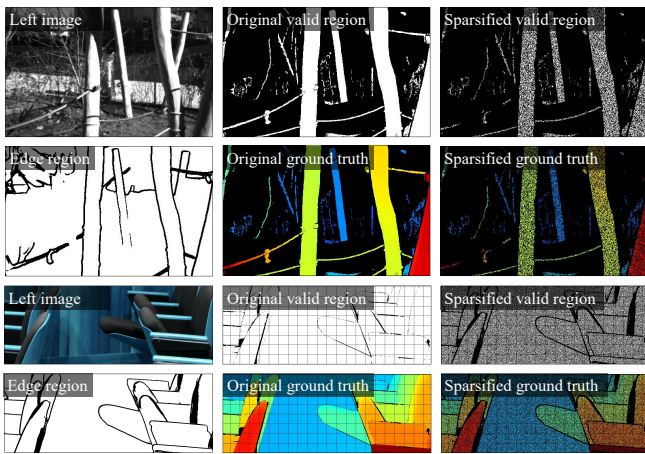


Fig. 11. Visualization of ground truth sparse process for ETH3D and Middbury 2014. First, we predict the edge map using the edge estimator proposed in Section IV-F1. Then, we remove the pixels in the edge region of the ground truth and randomly remove the pixels in the non-edge region with a probability of 0.5.

tive results that highlight the disparities between predicted edge maps obtained from different inputs. Notably, when the concatenation of disparity and RGB image is directly employed as input, the misleading influence of object surface texture is significantly reduced. This outcome demonstrates the effectiveness of integrating disparity information in edge estimation. Based on this, we further optimize the inputs of the disparity and RGB images to achieve accurate estimation of object edges using a lightweight network containing only two residual blocks.

TABLE VII

DOMAIN ADAPTATION EVALUATION OF DAPE ON ETH3D. WE EXPERIMENT WITH THE PROPOSED DAPE ON THREE MODELS. ALL METHODS ARE FINE-TUNED ON THE SPARSIFIED GROUND TRUTH AND EVALUATED ON THE ORIGINAL GROUND TRUTH. ALL METHODS RUN 15 DISPARITY UPDATES DURING INFERENCE. GRAY: PERFORMANCE IS IMPROVED AFTER USING DAPE. **BOLD**: BEST.

Methods	DAPE	$> 1px$	$> 0.75px$	$> 0.25px$	EPE(px)
RAFT-Stereo	-	3.46	4.47	20.74	0.315
	$t=0.25$	3.14	4.29	20.65	0.257
	$t=0.5$	2.94	4.18	20.79	0.256
	$t=0.75$	3.21	4.32	20.76	0.252
	$t=1.0$	2.98	4.26	20.59	0.255
IGEV-Stereo	-	1.65	2.13	14.74	0.186
	$t=0.25$	1.61	2.12	14.65	0.182
	$t=0.5$	1.67	2.20	14.72	0.178
	$t=0.75$	1.68	2.18	14.90	0.178
	$t=1.0$	1.68	2.18	14.97	0.179
SR-Stereo	-	1.59	1.99	14.31	0.181
	$t=0.25$	1.52	1.97	14.23	0.177
	$t=0.5$	1.64	2.08	13.76	0.178
	$t=0.75$	1.66	2.09	13.74	0.174
	$t=1.0$	1.69	2.13	13.76	0.176

2) *Threshold for Edge Pseudo-label Generation*: As mentioned in Section III-C2, erroneous disparity estimation in ill-posed regions can lead to incorrect edge maps. We propose the use of threshold-based filtering to select pixels in non-edge region as pseudo-label. In this section, our focus is on exploring the threshold settings in different target domains. By doing so, we aim to analyze the impact of pseudo-label density on the adaptation of various domains. This analysis allows us to gain insights into the relationship between pseudo-label density and the effectiveness of DAPE.

Results on ETH3D: As mentioned in Section IV-A, we divide the ETH3D training pairs into two parts which are used

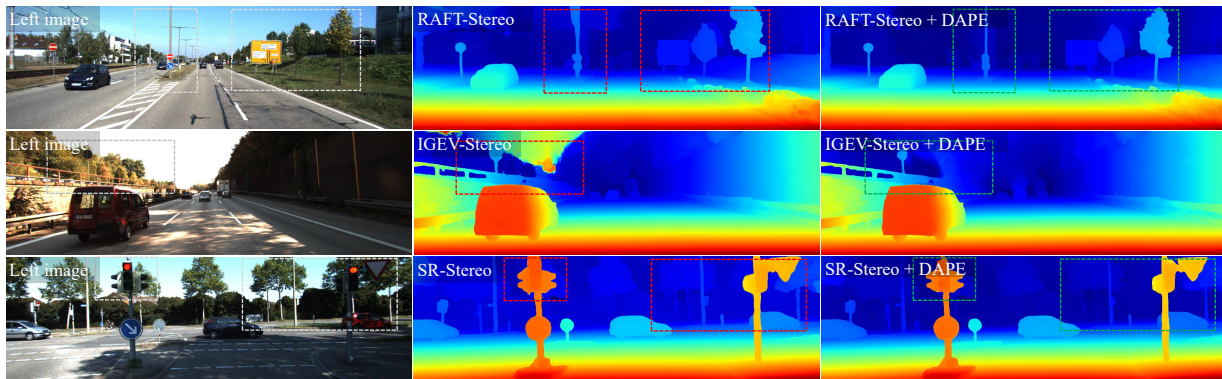


Fig. 12. Qualitative disparity estimation results of DAPE on KITTI test set. All methods run 15 disparity updates during inference. For RAFT-Stereo, the threshold t used for DAPE is 1, while for the other two models, it is 0.25.

TABLE VIII

DOMAIN ADAPTATION EVALUATION OF DAPE ON KITTI. WE EXPERIMENT WITH THE PROPOSED DAPE ON THREE MODELS. ALL METHODS RUN 15 DISPARITY UPDATES DURING INFERENCE. GRAY: PERFORMANCE IS IMPROVED AFTER USING DAPE. **BOLD**: BEST.

Methods	DAPE	3-noc	3-all	EPE-noc	EPE-all
RAFT-Stereo	-	1.17	1.37	0.483	0.507
	$t=0.25$	1.11	1.34	0.478	0.501
	$t=0.5$	1.14	1.38	0.479	0.506
	$t=0.75$	1.07	1.31	0.472	0.499
	$t=1.0$	1.07	1.29	0.474	0.499
IGEV-Stereo	-	0.99	1.20	0.448	0.472
	$t=0.25$	0.96	1.16	0.445	0.468
	$t=0.5$	0.96	1.17	0.445	0.471
	$t=0.75$	0.97	1.16	0.446	0.471
	$t=1.0$	0.97	1.17	0.446	0.469
SR-Stereo	-	0.98	1.20	0.443	0.471
	$t=0.25$	0.95	1.16	0.440	0.468
	$t=0.5$	0.97	1.17	0.442	0.465
	$t=0.75$	0.97	1.16	0.443	0.469
	$t=1.0$	0.98	1.16	0.446	0.469

for fine-tuning and evaluation respectively. To simulate the fine-tuning process on sparse ground truth, the ground truth of the part used for fine-tuning is randomly removed. Specifically, we remove the pixels in the edge region and randomly remove the pixels in the non-edge region with a probability of 0.5, as shown in Figure 11.

We utilize sparsified ground truth for model fine-tuning and the original ground truth for evaluation, ensuring a more accurate assessment of the model’s domain-adaptive performance. The experimental results are presented in Table VII. As the threshold t decreases in DAPE, the density of generated edge pseudo-labels decreases as well. When t is set to 0.25, all models exhibit performance improvement. This is due to the presence of reflective regions in some image pairs from ETH3D, which can lead to misleading edge map predictions. By using a smaller threshold, false edges are filtered out, resulting in more stable performance improvement. Figure 10 shows the qualitative results of DAPE for different models. It can be observed that our proposed DAPE effectively improves the performance of the model in the detail region.

Results on KITTI: Considering the limitation of the number of KITTI online leaderboard submissions, we have divided the KITTI training set into two parts, with a ratio of 4:1 for

TABLE IX

DOMAIN ADAPTATION EVALUATION OF DAPE ON MIDDLEBURY 2014. ALL METHODS ARE FINE-TUNED ON THE SPARSIFIED GROUND TRUTH AND EVALUATED ON THE ORIGINAL GROUND TRUTH. DUE TO THE LARGE DISPARITY RANGE OF MIDDLEBURY 2014, RAFT-STEREO RUNS 32 DISPARITY UPDATES DURING INFERENCE, WHILE THE OTHER TWO MODELS RUN 15 DISPARITY UPDATES. WE USE THE 2-PIXEL ERROR AS THE EVALUATION METRIC. GRAY: PERFORMANCE IS IMPROVED AFTER USING DAPE. **BOLD**: BEST.

Methods	DAPE	Full	Half	Quarter
RAFT-Stereo	-	12.85	8.14	7.56
	$t=0.25$	11.71	7.89	7.27
	$t=0.5$	11.56	7.89	7.02
	$t=0.75$	11.58	7.81	7.00
	$t=1.0$	11.47	7.84	6.87
IGEV-Stereo	-	11.72	5.14	5.00
	$t=0.25$	11.69	4.93	4.99
	$t=0.5$	11.38	4.93	4.98
	$t=0.75$	11.49	4.82	4.86
	$t=1.0$	11.53	4.92	4.85
SR-Stereo	-	11.06	4.99	4.65
	$t=0.25$	10.97	4.81	4.62
	$t=0.5$	10.90	5.00	4.61
	$t=0.75$	11.02	4.97	4.58
	$t=1.0$	11.01	4.97	4.56

fine-tuning the model and evaluation, respectively. The dataset provides sparse ground truth disparities obtained from lidar measurements. Notably, the upper regions of KITTI images primarily consist of sky and distant objects, where ground truth disparities are not available. Moreover, lidar performs poorly in the edge regions of objects, resulting in a lack of ground truth disparities for pixels in these areas. These factors lead to a mismatch between the accuracy ranking and the visualization on the KITTI online leaderboard. To ensure a more objective evaluation of the effectiveness of the proposed DAPE, we present the experimental results of DAPE on different models from both quantitative performance and visualization.

As shown in Table VIII, the implementation of DAPE with most threshold values leads to performance improvements in both non-occluded and overall regions for all three models. Notably, the RAFT-Stereo model benefits significantly from higher-density edge pseudo-labels. Despite the presence of some erroneous labels in high-density edge pseudo-labels, they provide more comprehensive edge information, which effectively complements the edge disparity update guidance in

RAFT-Stereo, especially considering its initial disparity is set to zero. Figure 12 showcases the qualitative results of DAPE on different models. Alongside enhancing the model’s performance in detailed regions, the proposed DAPE successfully mitigates disparity anomalies in textureless sky areas of the images.

Results on Middlebury: We use the additional 13 image pairs provided by Middlebury 2014 to fine-tune the models, and evaluate the domain adaptation performance using the original 15 training image pairs. Similar to the experiments conducted on ETH3D, we employ sparsified ground truth during the fine-tuning process, while relying on the original ground truth for evaluation, as shown in Figure 11.

To verify the performance of DAPE at different resolutions, we evaluate it on Middlebury 2014 with three different resolutions. The qualitative results of DAPE on Middlebury 2014 are presented in Table IX. Consistent with the conclusions from the previous two datasets, the implementation of DAPE with most threshold values leads to performance improvements of the three models. This outcome further confirms the generalizability and robustness of DAPE across different scenarios.

V. CONCLUSION

In this paper, we propose SR-Stereo, a novel stereo matching architecture. Our approach addresses the issue of distribution discrepancies across different datasets by predicting disparity clips. To enhance the accuracy of these disparity clips, we introduce a loss weight that is determined by the regression objective scale. Through extensive evaluations on datasets including SceneFlow, KITTI, Middlebury 2014, and ETH3D, we demonstrate that SR-Stereo achieves competitive performance in disparity estimation and state-of-the-art cross-domain generalisation performance. Moreover, we demonstrate that this stepwise regression architecture can be generalised to existing iteration-based methods to improve performance without changing the network structure.

Additionally, we propose a method called Domain Adaptation Based on Pre-trained Edge (DAPE) to address the issue of edge blurring in fine-tuned models with sparse ground truth. Specifically, we use the RGB image and the disparity predicted by the pre-trained stereo matching model to estimate the edge map of the target domain image. This eliminates the need for a complex edge estimation network. The generated edge map is then filtered to generate edge map background pseudo-labels. These pseudo-labels, along with the sparse ground truth disparity on the target domain, are used as supervision to jointly fine-tune the pre-trained stereo matching model. Experimental results at KITTI, Middlebury 2014, and ETH3D show that DAPE significantly improves the disparity estimation performance of the fine-tuned model, especially in untextured and detailed regions.

In our future work, we will delve deeper into advancing stepwise regression model to achieve more powerful cross-domain generalisation performance. In addition, we plan to design a more advanced edge estimator and develop an improved method for filtering edge pseudo-labels. These enhancements will further enhance the domain adaptation performance of

the fine-tuned model, enabling it to better handle challenging scenarios and improve disparity estimation performance.

REFERENCES

- [1] Y. Zhang, Z. Xiong, Z. Yang, and F. Wu, “Real-time scalable depth sensing with hybrid structured light illumination,” *IEEE Transactions on Image Processing*, vol. 23, no. 1, pp. 97–109, 2013.
- [2] S. Hou, M. Fu, and W. Song, “Joint learning of image deblurring and depth estimation through adversarial multi-task network,” *IEEE Transactions on Circuits and Systems for Video Technology*, 2023.
- [3] C. Feng, Z. Chen, C. Zhang, W. Hu, B. Li, and F. Lu, “Iterdepth: Iterative residual refinement for outdoor self-supervised multi-frame monocular depth estimation,” *IEEE Transactions on Circuits and Systems for Video Technology*, 2023.
- [4] H. Dai, X. Zhang, Y. Zhao, H. Sun, and N. Zheng, “Adaptive disparity candidates prediction network for efficient real-time stereo matching,” *IEEE Transactions on Circuits and Systems for Video Technology*, vol. 32, no. 5, pp. 3099–3110, 2021.
- [5] X. T. Nguyen, H. Kim, and H.-J. Lee, “An efficient sampling algorithm with a k-nn expanding operator for depth data acquisition in a lidar system,” *IEEE Transactions on Circuits and Systems for Video Technology*, vol. 30, no. 12, pp. 4700–4714, 2020.
- [6] Xu, B., Xu, Y., Yang, X., Jia, W., Guo, Y.: Bilateral grid learning for stereo matching networks. In: Proceedings of the IEEE/CVF Conference on Computer Vision and Pattern Recognition. pp. 12497–12506 (2021)
- [7] Li, Z., Liu, X., Drenkow, N., Ding, A., Creighton, F.X., Taylor, R.H., Unberath, M.: Revisiting stereo depth estimation from a sequence-to-sequence perspective with transformers. In: Proceedings of the IEEE/CVF international conference on computer vision. pp. 6197–6206 (2021)
- [8] Duggal, S., Wang, S., Ma, W.C., Hu, R., Urtasun, R.: Deeppruner: Learning efficient stereo matching via differentiable patchmatch. In: Proceedings of the IEEE/CVF international conference on computer vision. pp. 4384–4393 (2019)
- [9] Gu, X., Fan, Z., Zhu, S., Dai, Z., Tan, F., Tan, P.: Cascade cost volume for high-resolution multi-view stereo and stereo matching. In: Proceedings of the IEEE/CVF conference on computer vision and pattern recognition. pp. 2495–2504 (2020)
- [10] Yang, G., Zhao, H., Shi, J., Deng, Z., Jia, J.: Segstereo: Exploiting semantic information for disparity estimation. In: Proceedings of the European conference on computer vision (ECCV). pp. 636–651 (2018)
- [11] Liang, Z., Guo, Y., Feng, Y., Chen, W., Qiao, L., Zhou, L., Zhang, J., Liu, H.: Stereo matching using multi-level cost volume and multi-scale feature constancy. *IEEE transactions on pattern analysis and machine intelligence* **43**(1), 300–315 (2019)
- [12] Chang, J.R., Chen, Y.S.: Pyramid stereo matching network. In: Proceedings of the IEEE conference on computer vision and pattern recognition. pp. 5410–5418 (2018)
- [13] Guo, X., Yang, K., Yang, W., Wang, X., Li, H.: Group-wise correlation stereo network. In: Proceedings of the IEEE/CVF conference on computer vision and pattern recognition. pp. 3273–3282 (2019)
- [14] Xu, G., Cheng, J., Guo, P., Yang, X.: Attention concatenation volume for accurate and efficient stereo matching. In: Proceedings of the IEEE/CVF Conference on Computer Vision and Pattern Recognition. pp. 12981–12990 (2022)
- [15] Li, J., Wang, P., Xiong, P., Cai, T., Yan, Z., Yang, L., Liu, J., Fan, H., Liu, S.: Practical stereo matching via cascaded recurrent network with adaptive correlation. In: Proceedings of the IEEE/CVF conference on computer vision and pattern recognition. pp. 16263–16272 (2022)
- [16] Lipson, L., Teed, Z., Deng, J.: Raft-stereo: Multilevel recurrent field transforms for stereo matching. In: 2021 International Conference on 3D Vision (3DV). pp. 218–227. IEEE (2021)
- [17] Xu, G., Wang, X., Ding, X., Yang, X.: Iterative geometry encoding volume for stereo matching. In: Proceedings of the IEEE/CVF Conference on Computer Vision and Pattern Recognition. pp. 21919–21928 (2023)
- [18] X. Wang, G. Xu, H. Jia, and X. Yang, “Selective-stereo: Adaptive frequency information selection for stereo matching,” *arXiv preprint arXiv:2403.00486*, 2024.
- [19] Ma, Z., Teed, Z., Deng, J.: Multiview stereo with cascaded epipolar raft. In: European Conference on Computer Vision. pp. 734–750. Springer (2022)
- [20] Wang, H., Fan, R., Cai, P., Liu, M.: Pvstereo: Pyramid voting module for end-to-end self-supervised stereo matching. *IEEE Robotics and Automation Letters* **6**(3), 4353–4360 (2021)

- [21] Weinzaepfel, P., Lucas, T., Leroy, V., Cabon, Y., Arora, V., Brégier, R., Csurka, G., Antsfeld, L., Chidlovskii, B., Revaud, J.: Croco v2: Improved cross-view completion pre-training for stereo matching and optical flow. In: *Proceedings of the IEEE/CVF International Conference on Computer Vision*. pp. 17969–17980 (2023)
- [22] Zhao, H., Zhou, H., Zhang, Y., Chen, J., Yang, Y., Zhao, Y.: High-frequency stereo matching network. In: *Proceedings of the IEEE/CVF Conference on Computer Vision and Pattern Recognition*. pp. 1327–1336 (2023)
- [23] Shaked, A., Wolf, L.: Improved stereo matching with constant highway networks and reflective confidence learning. In: *Proceedings of the IEEE conference on computer vision and pattern recognition*. pp. 4641–4650 (2017)
- [24] Kim, S., Min, D., Kim, S., Sohn, K.: Unified confidence estimation networks for robust stereo matching. *IEEE Transactions on Image Processing* **28**(3), 1299–1313 (2018)
- [25] Chen, L., Wang, W., Mordohai, P.: Learning the distribution of errors in stereo matching for joint disparity and uncertainty estimation. In: *Proceedings of the IEEE/CVF Conference on Computer Vision and Pattern Recognition*. pp. 17235–17244 (2023)
- [26] Shen, Z., Dai, Y., Rao, Z.: Cfnets: Cascade and fused cost volume for robust stereo matching. In: *Proceedings of the IEEE/CVF Conference on Computer Vision and Pattern Recognition*. pp. 13906–13915 (2021)
- [27] Shen, Z., Song, X., Dai, Y., Zhou, D., Rao, Z., Zhang, L.: Digging into uncertainty-based pseudo-label for robust stereo matching. *IEEE Transactions on Pattern Analysis and Machine Intelligence* (2023)
- [28] Zhang, F., Qi, X., Yang, R., Prisacariu, V., Wah, B., Torr, P.: Domain-invariant stereo matching networks. In: *Computer Vision—ECCV 2020: 16th European Conference, Glasgow, UK, August 23–28, 2020, Proceedings, Part II 16*. pp. 420–439. Springer (2020)
- [29] Mayer, N., Ilg, E., Hausser, P., Fischer, P., Cremers, D., Dosovitskiy, A., Brox, T.: A large dataset to train convolutional networks for disparity, optical flow, and scene flow estimation. In: *Proceedings of the IEEE conference on computer vision and pattern recognition*. pp. 4040–4048 (2016)
- [30] Scharstein, D., Hirschmüller, H., Kitajima, Y., Krathwohl, G., Nešić, N., Wang, X., Westling, P.: High-resolution stereo datasets with subpixel-accurate ground truth. In: *Pattern Recognition: 36th German Conference, GCPR 2014, Münster, Germany, September 2-5, 2014, Proceedings 36*. pp. 31–42. Springer (2014)
- [31] Menze, M., Geiger, A.: Object scene flow for autonomous vehicles. In: *Proceedings of the IEEE conference on computer vision and pattern recognition*. pp. 3061–3070 (2015)
- [32] Geiger, A., Lenz, P., Urtasun, R.: Are we ready for autonomous driving? the kitti vision benchmark suite. In: *2012 IEEE conference on computer vision and pattern recognition*. pp. 3354–3361. IEEE (2012)
- [33] T. Wu, Z. Liu, Q. Huang, Y. Wang, and D. Lin, “Adversarial robustness under long-tailed distribution,” in *Proceedings of the IEEE/CVF conference on computer vision and pattern recognition*, 2021, pp. 8659–8668.
- [34] W. Wang, Z. Zhao, P. Wang, F. Su, and H. Meng, “Attentive feature augmentation for long-tailed visual recognition,” *IEEE Transactions on Circuits and Systems for Video Technology*, vol. 32, no. 9, pp. 5803–5816, 2022.
- [35] J. Scharcanski and A. N. Venetsanopoulos, “Edge detection of color images using directional operators,” *IEEE Transactions on Circuits and Systems for Video Technology*, vol. 7, no. 2, pp. 397–401, 1997.
- [36] C. Wei, J. Zhao, W. Zhou, and H. Li, “Semantic boundary detection with reinforcement learning for continuous sign language recognition,” *IEEE Transactions on Circuits and Systems for Video Technology*, vol. 31, no. 3, pp. 1138–1149, 2020.
- [37] Q. Zhang, S. Wang, X. Wang, Z. Sun, S. Kwong, and J. Jiang, “A multi-task collaborative network for light field salient object detection,” *IEEE Transactions on Circuits and Systems for Video Technology*, vol. 31, no. 5, pp. 1849–1861, 2020.
- [38] N. A. Valente, Z. Mao, and C. Niezrecki, “Holistically nested edge detection and particle filtering for subtle vibration extraction,” *Mechanical Systems and Signal Processing*, vol. 204, p. 110753, 2023.
- [39] Y. Ye, R. Yi, Z. Cai, and K. Xu, “Stedge: Self-training edge detection with multilayer teaching and regularization,” *IEEE Transactions on Neural Networks and Learning Systems*, 2023.
- [40] L. Liu, Z. Liu, A. Hou, X. Qian, and H. Wang, “Adaptive edge detection of rebar thread head image based on improved canny operator,” *IET Image Processing*, 2023.
- [41] Zhang, F., Prisacariu, V., Yang, R., Torr, P.H.: Ga-net: Guided aggregation net for end-to-end stereo matching. In: *Proceedings of the IEEE/CVF Conference on Computer Vision and Pattern Recognition*. pp. 185–194 (2019)
- [42] Zhang, Y., Chen, Y., Bai, X., Yu, S., Yu, K., Li, Z., Yang, K.: Adaptive unimodal cost volume filtering for deep stereo matching. In: *Proceedings of the AAAI Conference on Artificial Intelligence*. vol. 34, pp. 12926–12934 (2020)
- [43] C. C. Pham and J. W. Jeon, “Domain transformation-based efficient cost aggregation for local stereo matching,” *IEEE Transactions on Circuits and Systems for Video Technology*, vol. 23, no. 7, pp. 1119–1130, 2012.
- [44] Teed, Z., Deng, J.: Raft: Recurrent all-pairs field transforms for optical flow. In: *Computer Vision—ECCV 2020: 16th European Conference, Glasgow, UK, August 23–28, 2020, Proceedings, Part II 16*. pp. 402–419. Springer (2020)
- [45] Cho, K., Van Merriënboer, B., Gulcehre, C., Bahdanau, D., Bougares, F., Schwenk, H., Bengio, Y.: Learning phrase representations using rnn encoder-decoder for statistical machine translation. arXiv preprint arXiv:1406.1078 (2014)
- [46] Graves, A., Graves, A.: Long short-term memory. *Supervised sequence labelling with recurrent neural networks* pp. 37–45 (2012)
- [47] M. Sandler, A. Howard, M. Zhu, A. Zhmoginov, and L.-C. Chen, “Mobilenetv2: Inverted residuals and linear bottlenecks,” in *Proceedings of the IEEE conference on computer vision and pattern recognition*, 2018, pp. 4510–4520.
- [48] A. Krizhevsky, I. Sutskever, and G. E. Hinton, “Imagenet classification with deep convolutional neural networks,” *Communications of the ACM*, vol. 60, no. 6, pp. 84–90, 2017.
- [49] He, K., Zhang, X., Ren, S., Sun, J.: Deep residual learning for image recognition. In: *Proceedings of the IEEE conference on computer vision and pattern recognition*. pp. 770–778 (2016)
- [50] Schops, T., Schonberger, J.L., Galliani, S., Sattler, T., Schindler, K., Pollefeys, M., Geiger, A.: A multi-view stereo benchmark with high-resolution images and multi-camera videos. In: *Proceedings of the IEEE conference on computer vision and pattern recognition*. pp. 3260–3269 (2017)

Weiqing Xiao received the B.S. degree from SHENYUAN Honors College of Beihang University in 2022. He is currently pursuing the master’s degree in School of Electronic Information Engineering, Beihang University. His research interests include computer vision and 3D vision.